

RESEARCH

Open Access



Designing a multi-epitope universal vaccine for concurrent infections of SARS-CoV-2 and influenza viruses using an immunoinformatics approach

Shirin Mohammadipour^{1*}, Hadi Tavakkoli^{2*}, Seyedeh Narges Fatemi³, Aram Sharifi^{4*} and Peyman Mahmoudi⁴

Abstract

Background Severe acute respiratory syndrome coronavirus 2 (SARS-CoV-2) and influenza viruses share several conserved epitopes that can be utilized for the development of universal vaccines. Our previous research demonstrated that recombinant M2e-HA2 (Matrix-2 ectodomain-Hemagglutinin subunit 2) proteins derived from influenza elicited an immune response against the virus, suggesting their potential use in universal influenza vaccine formulations. Given the lack of a specific vaccine to address SARS-CoV-2 and influenza co-infections, this study aimed to design a universal vaccine using immunoinformatics methodologies.

Methods In this study, B-cell and T-cell epitopes were identified from the nucleocapsid (N) protein of SARS-CoV-2. Additionally, the N-terminal segments of M2e (SLLTEVET) and HA2 (GLFGAIAGF) from influenza were incorporated to construct a multi-epitope vaccine. Suitable linkers were designed, and human beta-defensin-2 was selected as an adjuvant. Further evaluations were conducted, focusing on key parameters such as stability, allergenicity, and antigenicity.

Results The major histocompatibility complex (MHC) class I and II binding epitopes exhibited broad population coverage for the vaccine on a global scale. The vaccine structure was found to interact with toll-like receptor 3 (TLR-3), and the docked conformation of the vaccine/TLR-3 complex demonstrated high stability during molecular dynamics (MD) simulations. The constructed vaccine exhibited thermal stability across cold, ambient, and human body temperatures. Additionally, in silico cloning of the vaccine candidate into the pET-28a(+) vector was performed to facilitate production within the *Escherichia coli* expression system.

*Correspondence:

Shirin Mohammadipour
mohammadipourshirin20@gmail.com
Hadi Tavakkoli
tavakkoli@uk.ac.ir
Aram Sharifi
A.sharifi@uok.ac.ir

Full list of author information is available at the end of the article



© The Author(s) 2025. **Open Access** This article is licensed under a Creative Commons Attribution-NonCommercial-NoDerivatives 4.0 International License, which permits any non-commercial use, sharing, distribution and reproduction in any medium or format, as long as you give appropriate credit to the original author(s) and the source, provide a link to the Creative Commons licence, and indicate if you modified the licensed material. You do not have permission under this licence to share adapted material derived from this article or parts of it. The images or other third party material in this article are included in the article's Creative Commons licence, unless indicated otherwise in a credit line to the material. If material is not included in the article's Creative Commons licence and your intended use is not permitted by statutory regulation or exceeds the permitted use, you will need to obtain permission directly from the copyright holder. To view a copy of this licence, visit <http://creativecommons.org/licenses/by-nc-nd/4.0/>.

Conclusion Overall, the findings suggest that the designed vaccine has the potential to serve as an effective universal vaccine and a promising strategy for controlling both Coronavirus disease 2019 (COVID-19) and influenza on a global scale.

Keywords SARS-CoV-2, Influenza, Universal vaccine, Multi-epitope design, Immunoinformatics, Molecular Docking

Introduction

COVID-19 and influenza are highly contagious viral diseases with significant mortality rates among infectious diseases. The recent COVID-19 pandemic has been classified as a global public health emergency by the World Health Organization (WHO), with over 776.8 million confirmed cases and approximately 7 million deaths reported worldwide as of December 2024. Similarly, influenza viruses continue to circulate globally, with an estimated 1 billion cases and 650,000 respiratory-related deaths reported annually, according to the WHO. Influenza poses a risk of severe illness or death, particularly among vulnerable populations, including the elderly, young children, pregnant women, and individuals with pre-existing medical conditions. In temperate regions, influenza epidemics primarily occur during the winter months, whereas in tropical regions, the disease may persist year-round [1, 2].

COVID-19 is caused by a novel coronavirus classified within the genus *Betacoronavirus*, specifically identified as SARS-CoV-2. The viral genome consists of a single-stranded positive-sense RNA that encodes at least six open reading frames (ORFs). Structural and accessory proteins are synthesized from subgenomic RNAs (sgRNAs). The key structural proteins of SARS-CoV-2 include the spike (S), nucleocapsid (N), membrane (M), and envelope (E) proteins [3].

In contrast, influenza viruses are categorized into types A, B, and C based on the antigenic properties of their surface glycoproteins. While all types can infect humans, only type A influenza is considered a significant pandemic threat. Influenza A virus belongs to the *Orthomyxoviridae* family and has a segmented genome comprising eight single-stranded RNA segments. These segments encode several essential proteins, including hemagglutinin (HA), neuraminidase (NA), polymerase proteins (PB1, PB2, and PA), membrane proteins (M1 and M2), nucleoprotein (NP), and non-structural proteins (NS1 and NS2). Notably, three of these proteins—HA, NA, and M2—are displayed on the surface of the viral particle [2, 4, 5].

Several antiviral agents, including remdesivir, oseltamivir, zanamivir, and amantadine, have been used in the treatment of COVID-19 and influenza; however, satisfactory therapeutic outcomes have often been difficult to achieve. The high transmissibility of these viruses, combined with the lack of effective medical countermeasures, highlights the necessity of vaccination as the most viable

strategy for controlling COVID-19 and influenza infections [2, 6, 7].

Currently, vaccines for COVID-19, such as mRNA vaccines (e.g., Pfizer-BioNTech and Moderna) and viral vector vaccines (e.g., AstraZeneca), have proven to be highly effective in preventing severe disease, hospitalization, and death. Similarly, seasonal influenza vaccines, including inactivated or live-attenuated vaccines, have played a crucial role in reducing the impact of influenza outbreaks. However, both types of vaccines face challenges, such as antigenic drift (for influenza) and the need for regular booster shots (for COVID-19), to maintain efficacy against evolving viral strains [5–7].

The development and production of vaccines for SARS-CoV-2 and influenza present multiple challenges, including antigenic shift, antigenic drift, mismatches, and the presence of heterologous circulating strains. To overcome these challenges, vaccine formulations should be based on conserved peptides, such as the N protein of the SARS-CoV-2 virus and the ectodomain of the matrix-2 protein (M2e) and HA2 of influenza viruses [8–10].

The N protein of SARS-CoV-2 exhibits a high degree of conservation, with a limited number of mutations, and plays a crucial role in various processes, including viral replication, mRNA transcription, N assembly, and viral egress. It is a highly immunogenic component, with its expression significantly upregulated following infection [11]. Notably, immunoglobulin G (IgG) antibody responses targeting the N protein have been detected in the sera of infected patients [12]. Furthermore, this protein is considered a promising target for T-cell stimulation in vaccination strategies. Research indicates that the C-terminal and central domains of the N protein are essential for inducing antibody responses after coronavirus infection [13].

The M2 protein of influenza is a transmembrane protein composed of a non-glycosylated ectodomain with 24 amino acids at the N-terminus, 54 amino acids at the C-terminus, and 19 amino acids embedded within the lipid membrane. The extracellular domain of the M2 protein, known as M2e, exhibits a high degree of conservation, with its N-terminal epitope (SLLTEVET) remaining stable across all subtypes of influenza A viruses [9, 13].

Additionally, the HA protein of influenza consists of two subunits, HA1 (approximately 324 amino acids) and HA2 (approximately 222 amino acids), and is expressed as a trimer on the viral particle. Research indicates that the HA2 sequence (GLFGAIAGF) represents a conserved

epitope with significant antigenicity. As a result, both M2e and HA2 are considered promising candidates for the development of universal influenza vaccines [9, 13].

Recent advances in computational vaccine design have provided innovative solutions for developing effective vaccines against infectious diseases. Computational tools enable the prediction of immunogenic epitopes, assessment of antigenicity and allergenicity, and modeling of vaccine-receptor interactions. These approaches have been widely used not only in infectious disease research but also in the design of therapeutic cancer vaccines [13, 14]. For instance, recent studies have successfully applied computational methodologies in the design of vaccines targeting both cancer and infectious diseases, demonstrating their potential for optimizing immunogenicity and stability in vaccine constructs [14].

Our previous research demonstrated that recombinant M2e-HA2 surface proteins elicit an immune response against the influenza virus, indicating their potential utility in the development of universal vaccines [9]. Given the absence of an effective vaccine to prevent concurrent infections of COVID-19 and influenza, the present study aimed to design a universal multi-epitope vaccine utilizing immunoinformatics methodologies to confer protection against the life-threatening effects of both COVID-19 and influenza. This vaccine incorporates multiple epitopes derived from the N protein of SARS-CoV-2, as well as the M2e and HA2 proteins of influenza viruses. Subsequently, molecular docking and dynamics simulations were employed to elucidate the molecular interactions and stability of the vaccine construct with the human immune receptor.

Materials and methods

Sequence retrieval and analysis of SARS-CoV-2/influenza proteins

The amino acid sequences of the M2 and HA2 proteins from the H9N2 subtype of influenza were retrieved from the UniProt database (<https://www.uniprot.org/uniprot/>) using the accession IDs A0A0S2RNU5 and A0A0S2RPB4, respectively. Additionally, the N protein sequence of SARS-CoV-2 was obtained using the accession ID P0DTC9.

The VaxiJen server (<http://www.ddg-pharmfac.net/vaxijen/VaxiJen/VaxiJen.html>) and AllerCatPro 2.0 (<https://allercatpro.bu.edu/>) were used to evaluate the antigenic and allergenic properties of the M2e, HA2, and N proteins. These amino acid sequences were then utilized in the design of a multi-epitope universal vaccine.

Identification of cytotoxic T lymphocyte (CTL), helper T lymphocyte (HTL), and B-cell receptor (BCR) epitopes

Epitope identification

The identification of CTL epitopes for the N protein of SARS-CoV-2 was performed using the NetCTL 1.2 server (<http://www.cbs.dtu.dk/services/NetCTL/>). This server predicts epitopes associated with supertypes A1, A2, A3, A24, A26, B7, B8, B27, B39, B44, B58, and B62, with a sensitivity of 0.89, specificity of 0.94, and an identification threshold of 0.50. The parameters for C-terminal cleavage and Transporter Associated with Antigen Processing (TAP) transport efficiency were set at 0.15 and 0.05, respectively. Following this, the immunogenicity and antigenicity of the identified epitopes were assessed using the Immune Epitope Database (IEDB) server (<http://tools.iedb.org/main/>) for class I immunogenicity and VaxiJen v2.0 for antigenicity evaluation. Additionally, the IEDB server was used to predict epitopes that bind to MHC class I molecules, employing the SMM method with an IC₅₀ threshold of less than 200.

HTL epitopes for the N protein of SARS-CoV-2 were identified using the IEDB MHC-II binding prediction tool (<http://tools.iedb.org/mhcii/>). A set of 15-amino-acid-long HTL epitopes was evaluated using the SMM_Align method to determine IC₅₀ values and percentile scores, which indicate binding affinity to MHC-II molecules. The analysis focused on human loci, specifically HLA-DP, HLA-DQ, and HLA-DR. Epitopes with IC₅₀ values below 200 and percentile scores under 1 were considered to have optimal binding affinity. The predicted HTL epitopes were further evaluated for their immunogenicity and antigenicity. For a more precise and up-to-date methodology in HTL epitope prediction, we have referred to the IEDB MHC-II workshop (<https://youtu.be/debeFK0dcK8?si=Z1c03cphy8Ix9wUS>) to enhance the prediction accuracy and reduce any potential errors or standard deviations in the prediction process.

B-cell epitopes for the N protein of SARS-CoV-2 were identified using the BepiPred server (<https://services.healthtech.dtu.dk/service.php?BepiPred-2.0>). These epitopes were selected based on their antigenic potential, focusing on surface exposure and other critical properties.

Epitope properties evaluation

After the identification of epitopes, their immunogenicity and antigenicity were assessed. For CTL and HTL epitopes, the IEDB server was used to predict immunogenicity, while VaxiJen v2.0 was employed to evaluate their antigenicity. The B-cell epitopes were similarly assessed using VaxiJen v2.0 and various tools from the IEDB server (e.g., Emini surface accessibility, Karplus & Schulz flexibility, Chou & Fasman beta-turn predictions, and Parker hydrophilicity).

The ToxinPred server (<http://crdd.osdd.net/raghava/toxinpred/>) was used to evaluate the potential toxicity of the predicted HTL, CTL, and BCR epitopes. This step is crucial for ensuring the safety of the proposed multi-epitope vaccine.

Assessment of vaccine population coverage

The population coverage of the developed vaccine was assessed using the IEDB server (<http://tools.iedb.org/population/>). This tool analyzes HLA alleles across different countries, ethnic groups, and regions, providing insights into the potential efficacy and broad applicability of the vaccine.

Construction of the SARS-CoV-2/influenza vaccine

The development of a multi-epitope universal vaccine involved the integration of influenza virus epitopes, specifically M2e and HA2, with SARS-CoV-2 epitopes, including CTL, HTL, and BCR. These components were assembled with an adjuvant and appropriate linkers to ensure the optimal spatial arrangement of epitopes under physiological conditions. To enhance the immunogenicity of the vaccine, human β -defensin-2 (PDB ID: 1FD3) was employed as an adjuvant and conjugated to the M2e epitope via the EAAAK linker. Subsequently, a structured linkage system was established: M2e was connected to HA2, HA2 to BCR, BCR to HTL, and HTL to CTL using the GSGSGS linker. Finally, the CTL epitopes were interconnected through the AAY linker.

Assessment of the SARS-CoV-2/influenza vaccine structure

The allergenicity of the developed vaccine was assessed using the AllergenFP v1.0 server (<http://ddg-pharmfac.nyu.edu/AllergenFP/index.html>), while its antigenicity was evaluated through VaxiJen. Subsequently, the ProtParam tool (<https://web.expasy.org/protparam/>), hosted by ExPASy and available through Biopython, was utilized to determine various physicochemical properties of the vaccine construct, including molecular weight, theoretical isoelectric point (pI), amino acid composition, atomic composition, estimated half-life, instability index, aliphatic index, and grand average of hydropathicity. Additionally, the Protein-Sol server (<https://protein-sol.manchester.ac.uk/>) was employed to analyze the solubility of the vaccine structure following its expression in *Escherichia coli* [15].

Simultaneously, the RaptorX-Property server (<http://raptorx.uchicago.edu/StructurePropertyPred/predict/>) was used to predict key structural properties of the vaccine, including solvent accessibility. RaptorX-Property is widely recognized for its accuracy in secondary structure prediction among bioinformatics tools. Furthermore, the secondary structure of the designed vaccine, including strands, helices, and coils, was predicted using PSIPRED v4.0 (<http://bioinf.cs.ucl.ac.uk/psipred/>).

Three-dimensional structure simulation and validation

The three-dimensional structure of the vaccine was simulated using a hierarchical assembly approach AlphaFold 3 server (<https://alphafold.ebi.ac.uk/>), which has been widely utilized in structural modeling studies [16]. The generated structure was further refined using the Galaxy-Refine server (<http://galaxy.seoklab.org/cgi-bin/submit.cgi?type=REFINE>), while loop and terminus optimizations were performed through the GalaxyLoop server (<http://galaxy.seoklab.org/cgi-bin/help.cgi?key=METHOD%26;type=LOOP>).

To ensure the accuracy and stability of the modeled structure, validation was conducted using the Ramachandran plot analysis (<https://saves.mbi.ucla.edu/>) and ProSA-web (<https://prosa.services.came.sbg.ac.at/prosa.php>) [17, 18].

Conformational B-Cell epitope prediction

Conformational or discontinuous B-cell epitopes were identified using the IEDB ElliPro server (<http://tools.iedb.org/ellipro/>). The vaccine structure was uploaded in PDB format, and epitope prediction was performed using the default parameters. ElliPro predicts conformational epitopes by analyzing multiple factors, including the protrusion index (PI score), the three-dimensional structure of the protein, approximated ellipsoidal shapes, and the spatial positioning of residues relative to the ellipsoid and the center of mass.

Binding pocket identification and molecular docking

To elucidate the interaction between the vaccine construct and the host immune receptor, molecular docking was performed, with the vaccine structure serving as the ligand and TLR-3 as the receptor. The binding pockets of TLR-3 were initially identified using the CastP server (<http://sts.bioe.uic.edu/castp/>), which employs computational geometry algorithms, such as shape discrete flows, to detect binding sites. Molecular docking was conducted using the HEX program (HEX[®] 8.0.0), a validated tool recognized in the CAPRI (Critical Assessment of Predicted Interactions; <http://capri.ebi.ac.uk/>) competition. The TLR-3 and vaccine structures were uploaded in PDB format for docking analysis. Following this, complex refinement and energy minimization were performed, and the conformation with the lowest energy score was selected.

To validate the docking assay, a self-docking procedure was conducted [19, 20]. In this approach, the PDB structure of 3ULV, which represents the crystal structure of human TLR-3 in complex with its ligand, was retrieved from the Protein Data Bank. After dissociating the ligand from the receptor, the binding conformation was reassessed through docking analysis.

Molecular dynamics simulation

Molecular dynamics (MD) simulations were conducted to investigate the molecular interactions and structural stability of the vaccine-TLR-3 complex over an extended simulation period. The simulations were performed using GROMACS version 5.4.1 with the AMBER force field [10, 23]. A dodecahedral box was constructed around the complex, which was subsequently solvated with TIP3P water molecules. To achieve system neutrality, Na⁺ or Cl⁻ ions were added as counterions. Electrostatic interactions were computed using the particle mesh Ewald (PME) method, and all molecular bonds were constrained using the LINCS algorithm.

The steepest descent algorithm was employed for energy minimization, ensuring an energetically favorable starting conformation. Following this, a 100 ps equilibration phase was carried out using the Leap-frog algorithm (time step: 0.002 ps). The system's pressure and temperature were controlled using the Parrinello-Rahman algorithm. Subsequently, the MD simulation was extended to 200 ns to capture long-range conformational changes and provide a more detailed assessment of complex stability.

To gain deeper insights into the stability and dynamic behavior of the vaccine-TLR-3 complex, several post-simulation analyses were performed including: Root-mean-square deviation (RMSD) to evaluate the overall structural stability of the complex; Root-mean-square fluctuation (RMSF) to analyze the flexibility of individual residues; Radius of gyration (Rg) to assess the compactness and folding behavior of the complex; Solvent-accessible surface area (SASA) to measure the solvent exposure of the complex; Hydrogen bond (H-bond) analysis to track the stability of interactions between the vaccine construct and TLR-3 over time; Principal component analysis (PCA) to identify dominant motions within the system and characterize large-scale conformational changes; Dynamic cross-correlation matrix (DCCM) analysis to examine correlated and anti-correlated motions between different regions of the complex; Free energy landscape (FEL) to explore conformational transitions and identify the most thermodynamically favorable states.

Furthermore, the thermal stability of the vaccine construct was evaluated at 4 °C, 25 °C, and 37.5 °C. For these simulations, all parameters-including equilibration and MD phases-were adjusted to 277.15 K (4 °C), 298.15 K (25 °C), and 310.65 K (37.5 °C), respectively.

The structures were visualized using PyMOL, Chimera, Grace, and Avogadro, and results were analyzed to determine the stability criteria of the vaccine-TLR-3 complex. The findings from these analyses were validated against previous molecular simulation studies, ensuring a robust evaluation of vaccine stability and interaction dynamics [21–23].

Computational cloning

Computational cloning was carried out through a three-step process: codon optimization, restriction enzyme identification, and cloning. In the first step, codon optimization was performed using the Codon Adaptation Tool (<http://www.jcat.de/>) to enhance the expression of the vaccine in the *E. coli* K12 strain. Next, the NEBcutter tool (<http://nc2.neb.com/NEBcutter2/>) was used to identify restriction enzymes that could cleave the sequence at a single site. Finally, the vaccine sequence was inserted into the multiple cloning sites of the pET-28a(+) plasmid using SnapGene software (GSL Biotech, snapgene.com), facilitating the expression of the vaccine candidate. The pET-28a(+) plasmid, which includes a poly-histidine tag (6xHis-tag), is a suitable vector for cloning and expressing recombinant vaccines.

Results

Structural properties of influenza and SARS-CoV-2 proteins

The amino acid sequences of the influenza M2 and HA2 proteins from the H9N2 subtype, along with the N protein of SARS-CoV-2, were evaluated for their antigenic and allergenic properties. The M2, HA2, and N proteins consist of 97, 222, and 419 amino acids, respectively, with approximate molecular masses of 11,302 Da, 25,063 Da, and 45,626 Da. Proteins with an antigenic predicted value exceeding 0.5 are considered to possess antigenic activity, making them suitable candidates for vaccine development. The calculated antigenic propensities for the M2, HA2, and N proteins were 0.426, 0.451, and 0.505, respectively. Subsequent analyses revealed that these proteins are non-allergenic. Consequently, these sequences were selected for the design of a multi-epitope universal vaccine.

CTL and HTL epitope identification

The CTL epitopes are critical for the activation of MHC class I-mediated cellular immunity. In this study, CTL epitopes of the N protein were identified using the NetCTL 1.2 server. The analysis revealed 104 nine-amino acid epitopes with combined threshold values exceeding 0.5 across all MHC class I supertypes. Following a comprehensive evaluation of various properties, including immunogenicity and antigenicity, eight CTL epitopes were selected (Table 1). Among these, three epitopes-GDAALALLL, SRIGMEVTP, and KKADETQAL-were prioritized for vaccine design. Notably, GDAALALLL is located within the central region of the N protein sequence, while SRIGMEVTP and KKADETQAL are situated in the C-terminal region.

HTL cells play a crucial role in the immune response by activating cytotoxic T cells and B cells, which are responsible for eliminating infected agents and secreting antibodies, respectively. In this study, the N protein

Table 1 Cytotoxic T-lymphocyte epitopes identified within the nucleocapsid protein of SARS-CoV-2

Sequences	Immunogenicity	Antigenicity	Toxicity	Position	MHC-I alleles bind (IC ₅₀ < 200)
QRNAPRITF	Yes	Yes	No	9–17	HLA-C*07:01; HLA-B*15:02; HLA-C*06:02; HLA-C*12:03; HLA-C*03:03; HLA-C*14:02
SSPDDQIGY	Yes	Yes	No	78–87	HLA-C*12:03; HLA-C*07:01
LSPRWYFYF	Yes	Yes	No	104–112	HLA-C*12:03; HLA-A*29:02; HLA-A*01:01
NPANNAIV	Yes	Yes	No	150–158	HLA-C*12:03; HLA-C*03:03
GDAALALLL	Yes	Yes	No	215–223	HLA-C*03:03; HLA-B*15:02; HLA-C*12:03
GTDYKHWPQ	Yes	Yes	No	295–304	HLA-C*12:03; HLA-C*05:01
SRIGMEVTP	Yes	Yes	No	318–326	HLA-C*12:03; HLA-C*03:03; HLA-C*07:01
KKADETQAL	Yes	Yes	No	374–383	HLA-C*03:03; HLA-C*12:03; HLA-B*15:02; HLA-B*39:01

Table 2 Evaluation of helper T-Lymphocyte epitopes derived from the nucleocapsid

Sequences	Immunogenicity	Antigenicity	Toxicity	Position	MHC-I alleles bind (IC ₅₀ < 200)
QIGYYRATRIRGG	Yes	Yes	No	83–97	HLA-DRB1*11:01;
NGGDAALALLLDRL	Yes	Yes	No	213–227	HLA-DRB4*01:01;
DAALALLLDRLNQL	Yes	Yes	No	216–230	HLA-DRB4*01:01, HLA-DRB1*03:01, HLA-DRB1*11:01,
GTWLYTGAIKLDDK	Yes	Yes	No	328–342	HLA-DRB1*07:01,
TWLYTGAIKLDDK	Yes	Yes	No	329–343	HLA-DRB1*07:01

Table 3 Identification of linear B-Lymphocyte epitopes within the nucleocapsid protein of the SARS-CoV-2 virus

Sequences	Position	Immunogenicity	Antigenicity	Surface exposed	Flexibility	Beta-turn	Hydrophilicity
ERSGARSKQRRPQGLP	27–42	Yes	Yes	Yes	Yes	Yes	Yes
SGARSKQRRPQGLPNN	31–46	Yes	Yes	Yes	Yes	Yes	Yes
NSTPGSSRGTSAPARMA	195–210	Yes	Yes	Yes	Yes	Yes	Yes

of SARS-CoV-2 was analyzed to predict HTL epitopes using the IEDB MHC-II binding prediction tool. HTL epitopes were identified based on an IC₅₀ score of less than 200 and a percentile rank below 1 for the HLA-DP, HLA-DQ, and HLA-DR loci. Among the identified HTL epitopes, those from the HLA-DR locus underwent further analysis, resulting in the selection of five epitopes (Table 2). Notably, one epitope (TWLYTGAIKLDDK) was prioritized for vaccine design due to its location in the C-terminal region.

Identification of BCR epitopes

B lymphocytes are integral to humoral immunity, primarily through the production of antibodies that target pathogenic agents. This study identified linear B-cell epitopes with a threshold of 0.5 and a length of 16 amino acids, utilizing the BepiPred and IEDB servers for evaluation. Subsequent sequence analysis revealed three B-cell epitopes (ERSGARSKQRRPQGLP, SGARSKQRRPQGLPNN, and NSTPGSSRGTSAPARMA) that met the criteria established by these servers. Furthermore, these epitopes exhibited properties of immunogenicity and antigenicity. The selected epitopes were further evaluated across various parameters, including surface exposure, flexibility, beta-turn prediction, and hydrophilicity (Table 3). Epitope regions must be located on the surface of proteins to facilitate recognition by antibodies. Additionally, a strong correlation exists between the

propensity of a peptide sequence to adopt a beta-turn conformation and its interaction with antibodies [24]. All selected B-cell epitopes demonstrated substantial scores across various predictive algorithms, including Karplus & Schulz flexibility, Emini surface accessibility, Chou & Fasman beta-turn prediction, and Parker hydrophilicity. Notably, one epitope, NSTPGSSRGTSAPARMA, was selected for vaccine design due to its position within the central region of the N protein, which is identified as an immunogenic domain.

Population coverage of the vaccine

The assessment of vaccine population coverage was conducted in light of the widespread occurrence of COVID-19 and influenza infections globally. This evaluation involved selected T-cell epitopes, comprising three CTL epitopes and one HTL epitope, along with their corresponding human leukocyte antigen (HLA) alleles and combined scores for MHC classes I and II. The findings indicate that the developed vaccine achieves a population coverage of 93.47% worldwide. Notably, the highest coverage was recorded in England at 96.1%, while the lowest coverage was observed in Bolivia at 42.24% and Pakistan at 64.55%. Detailed information regarding population coverage is presented in Fig. 1.

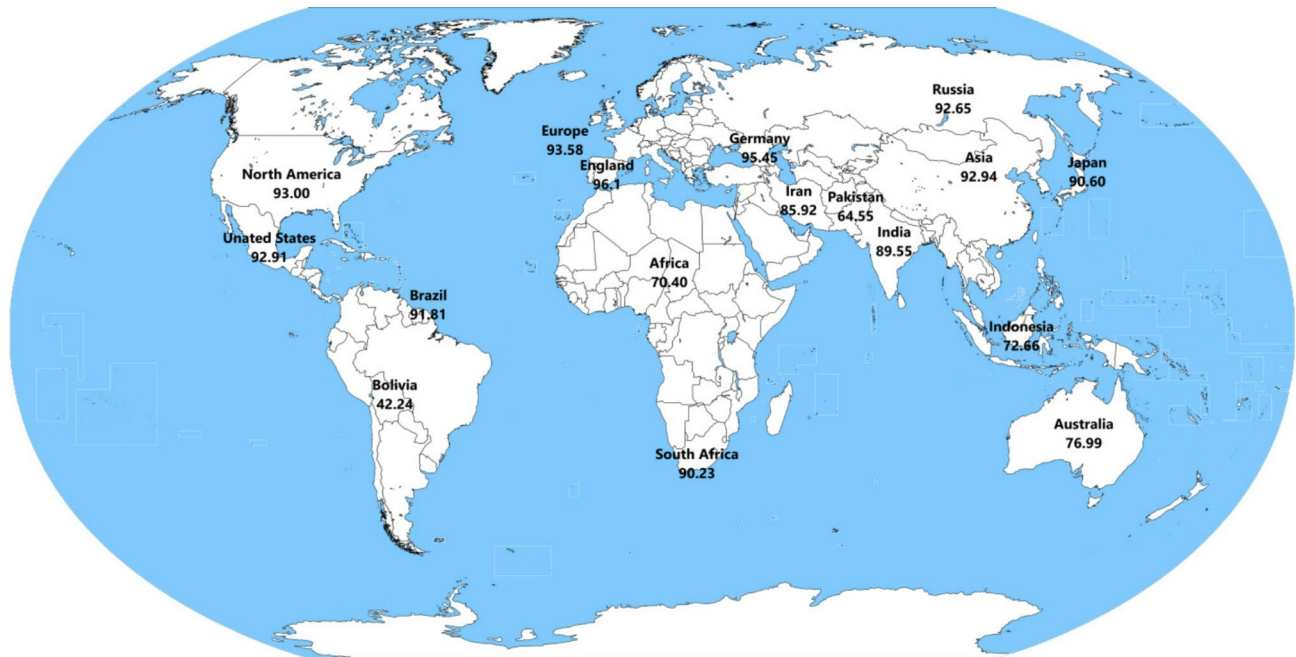


Fig. 1 Population coverage of the developed vaccine, illustrating T-cell epitopes alongside their respective MHC class I and II scores

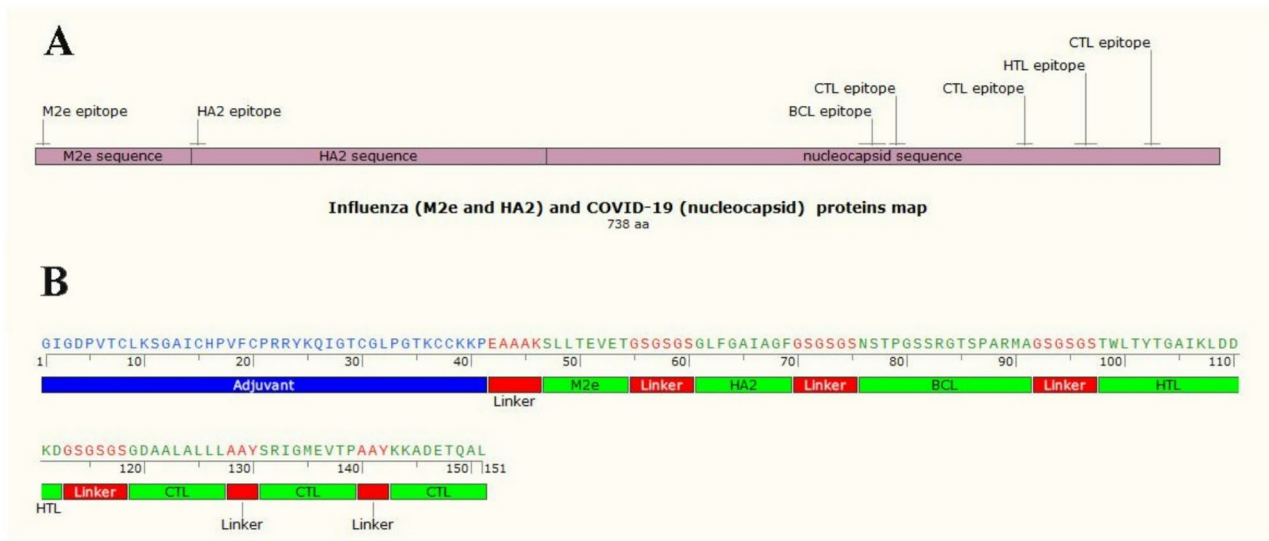


Fig. 2 Design of the multi-epitope universal vaccine. **(A)** The vaccine incorporates proteins from SARS-CoV-2 (N) and influenza (M2e and HA2), along with their associated epitopes. **(B)** The epitopes, comprising one M2e and one HA2, as well as three CTL, one HTL, and one BCR, were integrated utilizing appropriate adjuvants and linkers

Construction of the universal vaccine

The multi-epitope universal vaccine was constructed by assembling epitopes from SARS-CoV-2 (three CTL, one HTL, and one BCR epitope) and influenza (one M2e and one HA2 epitope) using appropriate linkers (Fig. 2). To enhance the immunogenicity of the designed vaccine, a specific adjuvant, human β -defensin-2 consisting of 41 amino acids, was incorporated. The EAAAK linker was used to connect the adjuvant with the influenza M2e epitope, preventing any interaction between the vaccine

structure and the adjuvant. Concurrently, the M2e epitope was linked to the BCR, the BCR to the HTL, and the HTL to the CTL epitopes using the GSGSGS linker, which facilitates conformational flexibility while preserving functional integrity. Additionally, the AAY linker was employed to maintain the structural connection between the CTL epitopes, thereby enhancing the potential for antigen presentation. The overall vaccine structure comprises 151 amino acids, integrating one adjuvant and seven epitopes interconnected by linkers.

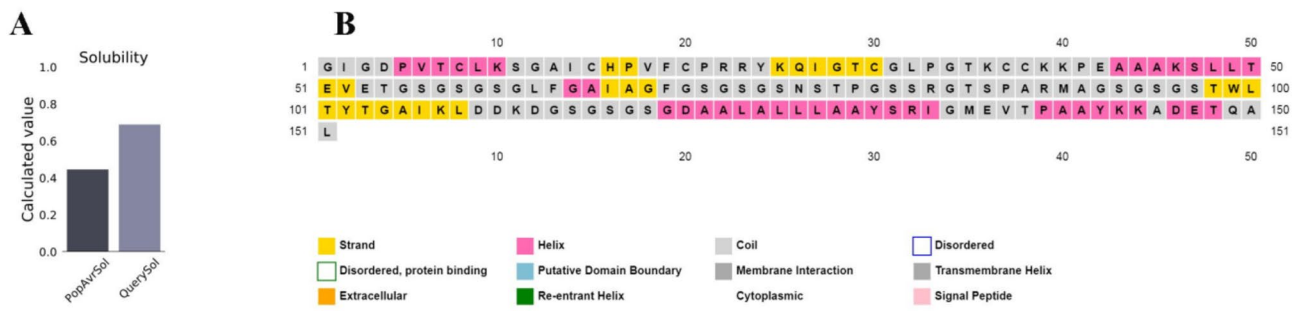


Fig. 3 Evaluation of the vaccine structure, emphasizing (A) solubility assessment and (B) conformational analysis

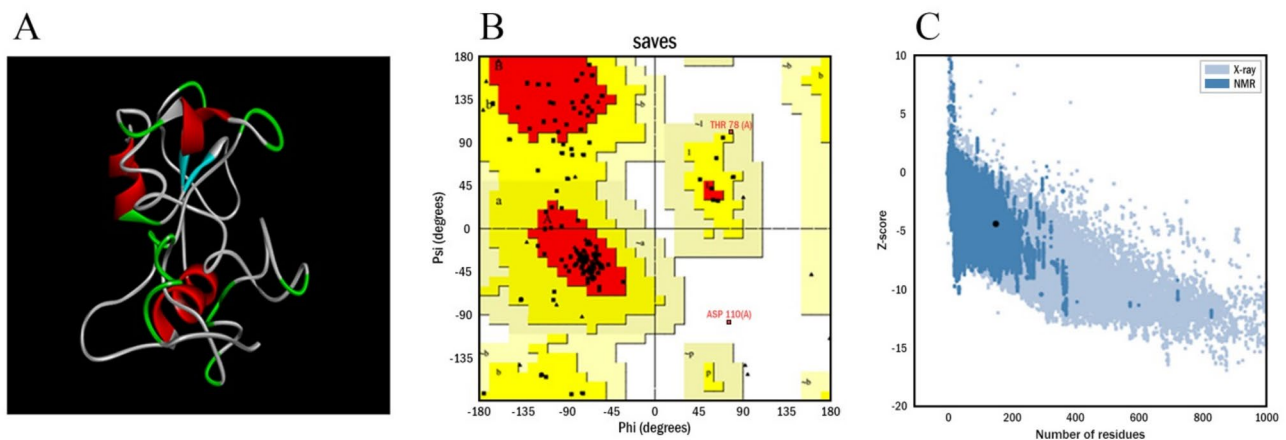


Fig. 4 Simulation and validation of the vaccine structure. (A) Three-dimensional conformation of the vaccine. (B) Ramachandran plots depicting the simulated model. (C) Screenshot illustrating the ProSA-web z-score plot

Vaccine evaluation

An effective vaccine must elicit both cellular and humoral immune responses against pathogenic agents, a characteristic known as immunogenicity. The vaccine developed in this study demonstrates significant antigenic activity, with an antigenic value of 0.592, as calculated using the VaxiJen server. Furthermore, the AllergenFP v1.0 server confirmed that the vaccine construct is non-allergenic. The ExPASy server was subsequently used to evaluate the physical and chemical parameters of the vaccine, yielding the following results: molecular weight = 14.92 kDa, theoretical isoelectric point (pI) = 8.78, total number of negatively charged residues (Asp + Glu) = 11, total number of positively charged residues (Arg + Lys) = 15, and total number of atoms = 2076. The estimated half-lives of the vaccine in mammalian reticulocytes (in vitro), yeast, and *E. coli* were found to be 30 h, greater than 20 h, and greater than 10 h, respectively, indicating the vaccine’s stability. The instability index was determined to be 23.88, classifying the vaccine structure as stable. The aliphatic index and grand average of hydropathicity were calculated to be 66.09 and -0.117, respectively, suggesting the vaccine’s thermostable and hydrophilic characteristics. Additionally, the vaccine structure demonstrated solubility upon expression, with a solubility value of

0.689 obtained from the Protein-Sol server (Fig. 3A). As shown in Fig. 3A, the scaled solubility value (QuerySol) represents the predicted solubility, suggesting favorable solubility for the vaccine construct. The population average for the experimental dataset (PopAvrSol) is 0.45, indicating that any scaled solubility value exceeding 0.45 is expected to exhibit greater solubility than the average soluble *E. coli* protein within the experimental solubility dataset. Simultaneously, the solvent accessibility of the vaccine structure was assessed using the RaptorX server. The results indicated that 80% of the residues were exposed, 12% were classified as medium accessibility, and 8% were buried. Additionally, the secondary structure of the vaccine was predicted using the PSIPRED 4.0 server, revealing that the vaccine structure comprises 15.89% strands, 26.49% helices, and 57.61% coils (Fig. 3B).

Three-dimensional structure simulation and validation

The three-dimensional conformation of the vaccine was simulated. A total of five models with varying C-scores were generated, with the optimal score of -4.15 identified. The resulting model was then refined to achieve a high-quality conformation approximating the native state, employing the GalaxyRefine server (Fig. 4A). The refined conformation was subsequently evaluated using

Table 4 Identification of conformational B-cell epitopes derived from the SARS-CoV-2/influenza vaccine

No.	Residues	Score	Number of residues
1	S114, G115, S116, G117	0.634	4
2	L108, D109, A: D110, K111, D112, A: A124, L125, L126, A: L127, A128, A129, Y130, I133, G134, A: M135, E136, T138, A: P139, A140, A141, Y142, K143, K144, A145, D146, E147, T148, Q149, A150, L151	0.628	30
3	G1, I2, G3, D4, T7, C8, K10, S11, G12, A13, I14, C15, H16, P17, V18, F19, C20, P21, R22, K25, Q26, I27, G28, T29, _: C30, P33, G34, T35, K36, C37, C38, K39, K40, P41, E42, A43, A44, A45, K46, S47, A105	0.716	41

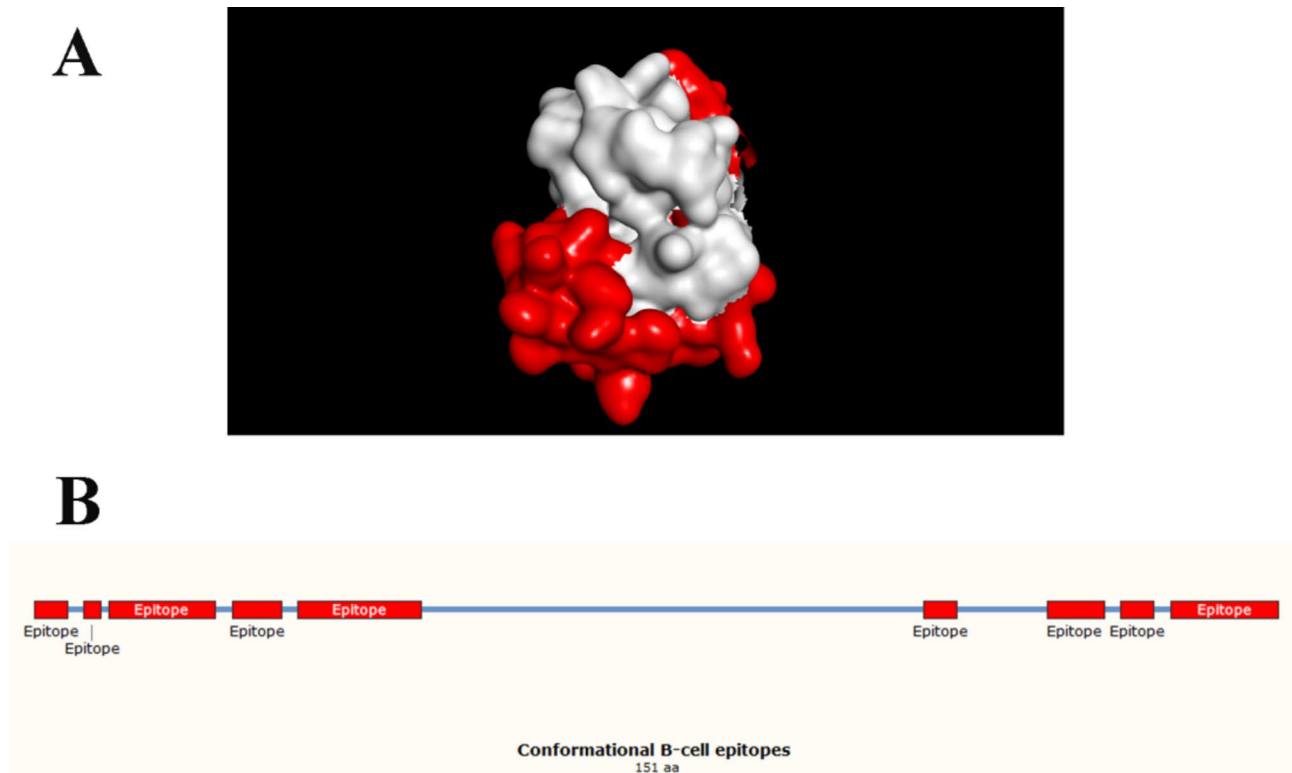


Fig. 5 Conformational B-Cell epitopes. (A) Predicted conformational epitopes indicated in red. (B) Locations of epitopes within the vaccine sequences

the Ramachandran plot, a key tool for assessing protein conformations. The analysis revealed that 98.2% of residues were located within favored and allowed regions (Fig. 4B). Following this, the simulated conformation was further assessed using the ProSA-web server to calculate the Z-score. The Z-score serves as an indicator of the overall quality of the model and can be used to determine whether the input structure aligns with the range typically observed for native proteins of comparable size. As shown in Fig. 4C, the Z-score of the simulated vaccine is -4.33, which is consistent with the range of NMR structures. Therefore, the obtained data supports the expectation of a high-quality vaccine conformation for subsequent evaluations.

Identification of conformational B-cell epitopes

Conformational B-cell epitopes are characterized by their spatial proximity within the three-dimensional structure

of proteins, despite being discontinuous in the linear protein sequence. In this study, conformational B-cell epitopes were systematically screened using the IEDB server. A range of conformational epitopes was identified, as detailed in Table 4 and illustrated in Fig. 5. The epitope scores, as presented in Table 4, ranged from 0.628 to 0.716, with epitope sizes varying from 4 to 41 residues. Notably, the highest-scoring epitope consisted of a 41-residue segment, achieving a score of 0.716. The identification of conformational B-cell epitopes within the vaccine structure suggests that the designed vaccine has the potential to elicit appropriate antibody responses following vaccination.

Molecular docking

Molecular docking was conducted using HEX to assess the interaction between the designed vaccine and TLR-3 (Fig. 6A). The lowest binding energy score of the

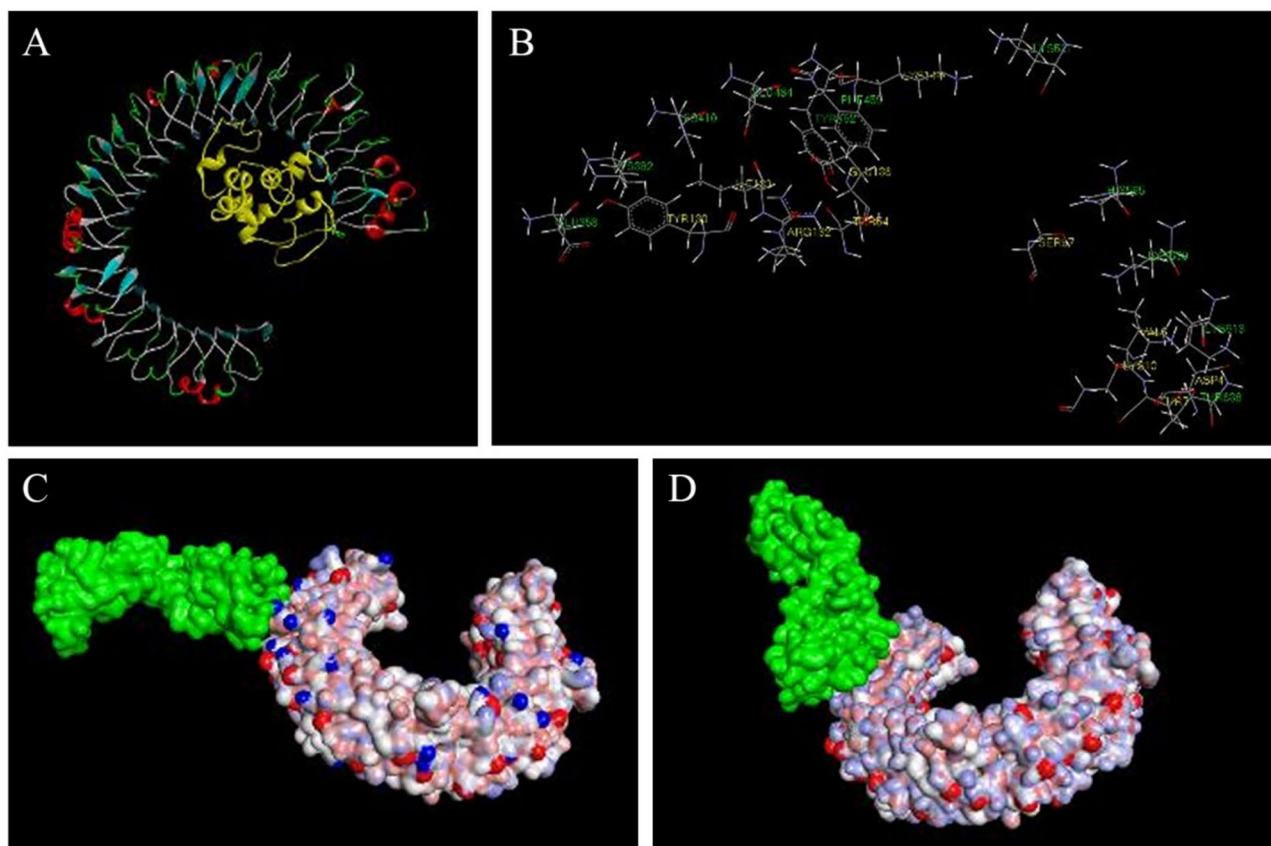


Fig. 6 Docking and self-docking results. **(A)** Docking analysis between the vaccine construct (ligand) and TLR-3 (receptor). **(B)** Identification of interacting residues between the vaccine and TLR-3. **(C)** and **(D)** Stages of self-docking; **(C)** Structure of 3ULV (the crystal structure of human TLR-3 in complex with its ligand). **(D)** The specific ligand of 3ULV (green) docked with its receptor in the correct orientation

ligand-receptor interaction was calculated as -393.61 kJ/mol. Lower binding energy values indicate stronger and more stable interactions, suggesting that the vaccine construct exhibits a high affinity for TLR-3. Key interacting residues were identified using Discovery Studio, revealing critical hydrogen bonding and hydrophobic interactions between vaccine residues (Asp4, Val6, Thr7, Lys10, Thr54, Ser97, Tyr130, Arg132, Ile133, Glu136, and Lys144) and TLR-3 residues (Glu358, Lys382, His410, Glu434, Phe459, Tyr462, Lys531, His565, Lys589, Lys613, and Thr638) (Fig. 6B). These interactions indicate that the vaccine construct effectively engages with immune receptors, potentially eliciting a robust immune response.

To validate the docking results, a self-docking experiment was performed using the native ligand of the TLR-3 complex (PDB ID: 3ULV), which correctly docked into the receptor's binding site, reinforcing the reliability of the docking approach. Similar studies have demonstrated that vaccines with strong TLR interactions exhibit enhanced immunogenicity, as seen in the research on computationally designed vaccines against SARS-CoV-2 [25].

Stability analysis during molecular dynamics simulation

MD simulations were performed to evaluate the stability of the vaccine-TLR-3 complex over a 1000 ps simulation period in an aqueous environment (Fig. 7A). The results from the MD simulations were analyzed through trajectory analysis to evaluate the stability of the complex. Assessments included RMSD, Rg, hydrogen bond formation, and binding energy calculations [26, 27].

The RMSD analysis demonstrated that the complex initially exhibited minor fluctuations but stabilized after 140 ps, with an average RMSD value of 0.495 nm. A stable RMSD suggests that the vaccine construct maintained structural integrity throughout the simulation (Fig. 7B).

The Rg serves as an indicator of protein compactness. For the vaccine-TLR-3 complex, the average Rg was 1.61 nm (Fig. 7C), with fluctuations of less than 0.06 nm. Throughout the MD simulation, the Rg of the vaccine-TLR-3 structure remained consistently close to the average value, which was lower than that of the initial structure. The relatively stable Rg values suggest that the structure maintained stability and compactness after 140 ps.

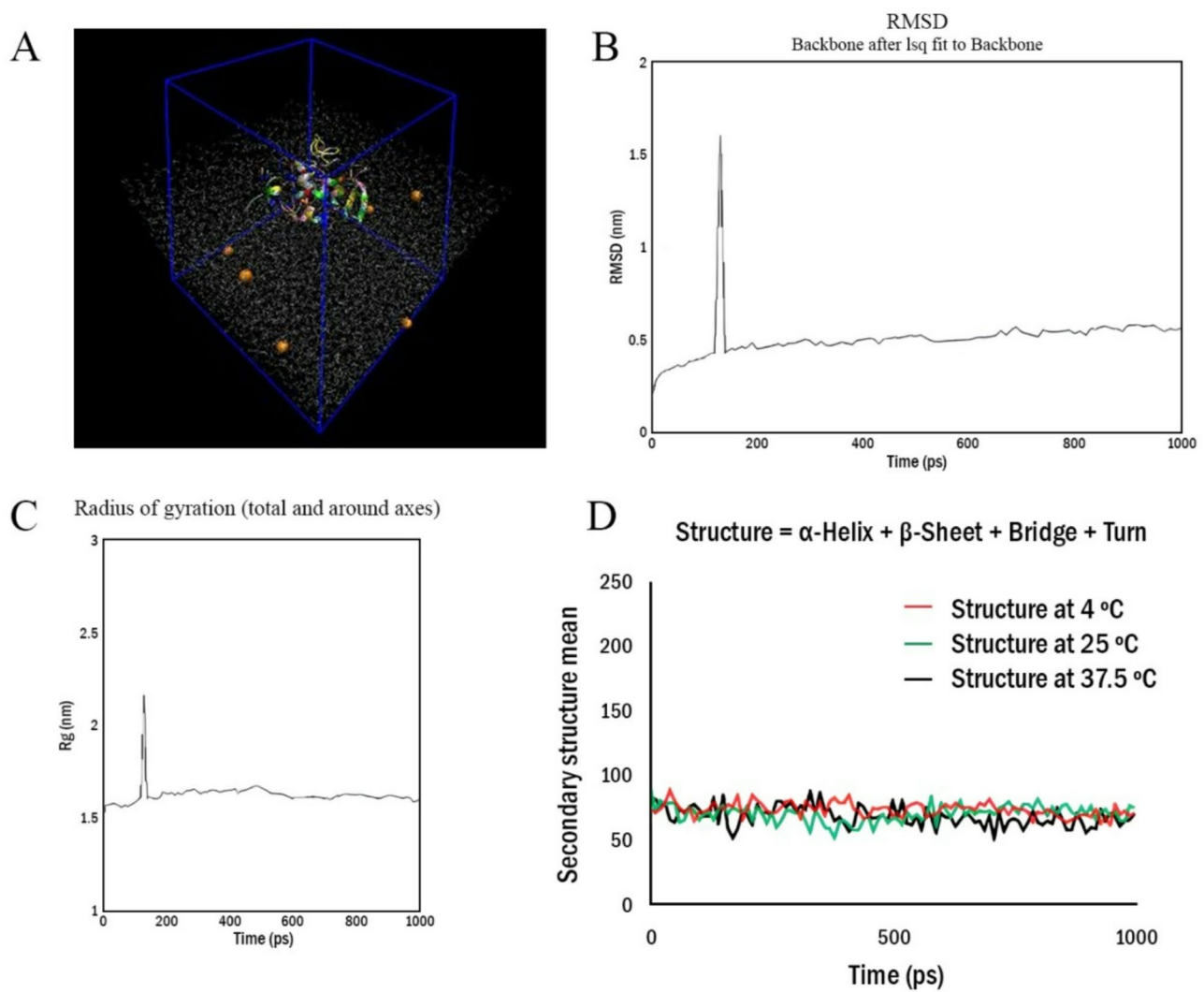


Fig. 7 Molecular Dynamics Simulations. Panel (A) illustrates the docked complex of the vaccine and TLR-3, solvated in TIP3P water, with sodium ions represented in orange. Panels (B) and (C) present the root RMSD and radius of gyration values, respectively. Panel (D) highlights the stable maintenance of the overall secondary structural pattern of the vaccine across varying temperatures (4 °C, 25 °C, and 37.5 °C) throughout the simulation

Table 5 The calculated binding free energy components for the vaccine-TLR-3 complex using the MM-PBSA method

	Van der Waals energy (kJ/mol)	Electrostatic energy (kJ/mol)	Polar solvation energy (kJ/mol)	SASA energy (kJ/mol)	Binding free energy (kJ/mol)
Initial structures	-153.89	-339.70	336.92	-23.06	-179.73
Stable structures	-166.73	-409.67	341.53	-24.61	-259.48

Hydrogen bond analysis showed an increase in hydrogen bonding between the vaccine and TLR-3 over time, with an initial average of 1.5 hydrogen bonds increasing to 5 bonds in the stable trajectory. Strong hydrogen bonding is crucial for maintaining molecular interactions and enhancing vaccine-receptor binding affinity.

The binding free energy between the vaccine and TLR-3 in both the initial and stable trajectory structures was evaluated using the Molecular Mechanics-Poisson

Boltzmann Surface Area (MM-PBSA) method [28]. The calculations included van der Waals, electrostatic, polar solvation, and non-polar solvation energies, with the results summarized in Table 5. The average binding free energy of the stable complex was -259.48 kJ/mol, significantly lower than the initial complex (-179.73 kJ/mol). The dominant electrostatic interactions suggest strong receptor engagement, consistent with findings in previous studies on viral vaccine docking [29].

Additionally, the reduction in solvation energy (SASA) relative to the initial structure indicated an increase in the compactness of the complex, corroborating the findings related to the Rg. In the preceding analysis, various evaluations were conducted to assess the structural stability of the vaccine-TLR-3 complex, comprising the vaccine construct and the host immune receptor, throughout the MD simulations. Additionally, the thermal stability of the vaccine construct was examined at varying temperatures of 4 °C, 25 °C, and 37.5 °C. This assessment involved analyzing the compactness of the secondary structure of the vaccine construct using the DSSP program [30].

The DSSP program was used to evaluate secondary structure composition, revealing that the overall structure remained consistent, suggesting the vaccine construct is thermally stable across physiological conditions (Fig. 7D). Distinct colors were employed to differentiate the secondary structures corresponding to the respective temperatures. The docking and MD simulation results support the strong interaction and stability of the vaccine construct with TLR-3, highlighting its potential effectiveness in eliciting an immune response. Comparisons with similar studies emphasize the importance of receptor-binding affinity and structural stability in vaccine design. These findings reinforce the promising nature of the designed vaccine and its potential for further *in vivo* validation.

Computational cloning and confirmation

Codon optimization of the vaccine construct was performed using the JCat server. The optimized DNA sequence of the vaccine consisted of 453 nucleotides with a GC content of 54.30%. Since the optimal GC content range is between 30% and 70%, these findings suggest a high likelihood of successful vaccine expression in a bacterial host. Additionally, XhoI and NdeI restriction sites were incorporated at the C-terminus and N-terminus of the optimized DNA, respectively, and these sequences were integrated into the multiple cloning sites of the pET-28a(+) plasmid. The final construct is illustrated in Fig. 8. The SnapGene software was employed to validate the cloning assay by simulating an agarose gel. Based on this, two prominent bands were observed, measuring approximately 5.5 kb (plasmid) and 0.5 kb (insert) after enzymatic digestion with XhoI and NdeI (data not shown). These sizes closely correspond to the calculated molecular weights of the pET-28a(+) plasmid and the engineered vaccine, respectively.

Discussion

In recent years, vaccination has emerged as a promising strategy for addressing viral diseases, notably COVID-19 and influenza [4, 7]. These viral infections can cause a wide range of illnesses, from mild to severe, with the

potential to lead to hospitalization and mortality on a global scale [2]. Given the limited efficacy of pharmacological treatments, there has been a concerted international effort to develop viable vaccines against SARS-CoV-2 and influenza. Currently, various vaccine candidates, including vector-based vaccines, subunit vaccines, mRNA vaccines, and peptide-based vaccines, are in various stages of preclinical and clinical trials [8, 26].

Epitope-based vaccines represent a promising strategy that uses short synthetic peptides to elicit immune responses [31]. These synthetic peptides include both B-cell and T-cell epitopes. In comparison to currently available vaccines, particularly live-attenuated vaccines, epitope-based vaccines offer several advantages, including reduced risk of causing disease, a simpler production process, and the potential for more targeted immune responses. Live-attenuated vaccines, although effective, can present challenges related to safety, especially in immunocompromised individuals, and are generally more complex to manufacture and store [32]. Epitope-based vaccines, by contrast, do not carry the same risks as live vaccines, as they only use selected portions of the pathogen's protein structure. However, one disadvantage is the potential for limited immunogenicity when compared to live-attenuated vaccines, which expose the immune system to a more comprehensive array of viral proteins. Additionally, epitope-based vaccines may require the use of adjuvants to enhance immune responses and achieve effective protection, further complicating their formulation [33].

Traditional experimental methods for screening immunogenic epitopes can be prohibitively expensive and time-consuming. As a result, immunoinformatics techniques have emerged as a valuable alternative. Immunoinformatics encompasses epitope prediction, molecular docking, MD simulations, and population coverage analysis. To address the antigenic variability of viruses, conserved regions of viral peptides are targeted to identify effective epitopes. The immunoinformatics approach has been extensively utilized in the design of novel vaccines for SARS-CoV-2 and influenza [8, 34, 35].

However, one limitation of epitope-based vaccines is their reliance on specific epitopes that may not be universally conserved across viral strains. This is especially relevant in the context of rapidly mutating viruses like influenza and SARS-CoV-2, where viral variants may carry mutations in the epitopes targeted by the vaccine. The emergence of new variants could reduce the efficacy of the vaccine, as the immune response may not be as robust against the altered epitopes. This issue has been observed in various studies where the immunogenicity of epitopes in new variants of the virus has been compromised. Therefore, it is critical to continuously monitor

Created with SnapGene®

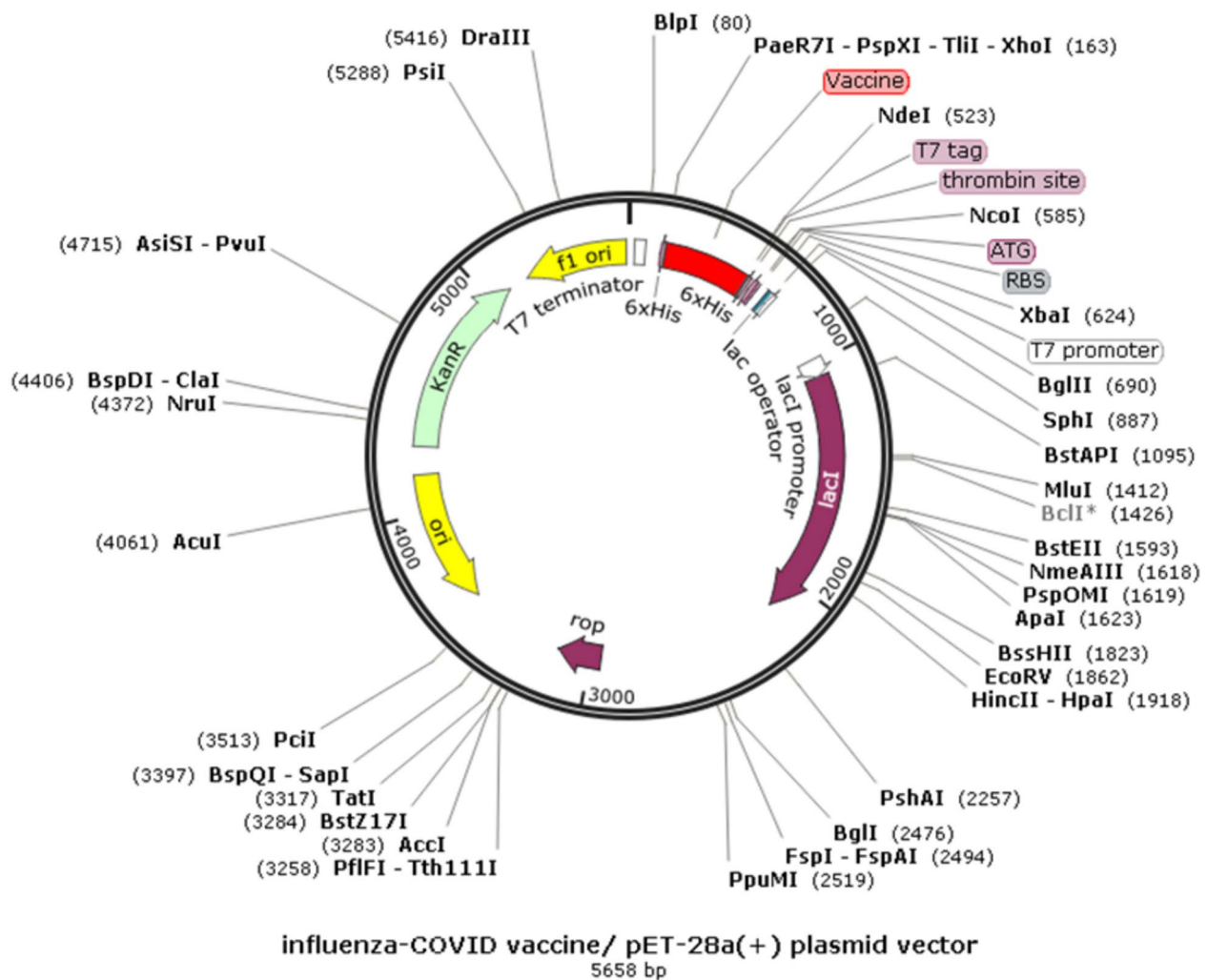


Fig. 8 Computational cloning process of the vaccine candidate; displays the gene sequence of the constructed vaccine, highlighted in red, which has been cloned into the pET-28a(+) vector

viral evolution and update epitope-based vaccines to account for new variants [36].

In this study, we employed immunoinformatics techniques for vaccine development. Numerous studies indicate that the N protein of the coronavirus is a conserved and highly immunogenic component [11]. The C-terminal and central regions of this protein play a significant role in eliciting antibody responses against coronavirus infection. Additionally, the N protein of SARS-CoV-2 exhibits antigenic properties while lacking allergenic activity, making it a suitable candidate for vaccine development [10]. Similarly, the M2e and HA2 proteins of influenza are conserved across various subtypes of influenza A and demonstrate immunogenic potential [14]. In the present study, the M2e (SLLTEVET) and HA2 (GLFGAIAGF) epitopes were selected for the design of

a universal vaccine. Notably, these epitopes were previously shown to be immunogenic in our in vivo experiments [9].

Vaccinal epitopes must effectively activate CTLs, HTLs, and BCRs to facilitate the release of various cytokines and antibodies, ultimately leading to the elimination of pathogenic agents. In this context, CTL, HTL, and BCR epitopes derived from the SARS-CoV-2 N protein were utilized to stimulate both cellular and humoral immune responses. The selection of T-cell epitopes was based on multiple criteria, including immunogenicity, antigenicity, allergenicity, toxicity, positional context, and the number of binding alleles for MHC class I and II. Concurrently, the B-cell epitope was chosen according to parameters such as immunogenicity, surface accessibility, antigenicity, flexibility, and hydrophilicity. Ultimately, three CTL epitopes, one HTL epitope, and one BCR

epitope were identified from the N protein of the SARS-CoV-2 virus. Notably, the immunogenicity of the selected CTL epitopes has been documented in prior studies [10, 37, 38]. Recent studies have similarly identified immunogenic epitopes from the N protein, such as those targeting MHC class I and II binding sites, which support the broad applicability of this protein in vaccine development. Furthermore, the chosen HTL epitope has been utilized in recent research to develop vaccine candidates for SARS-CoV-2 [39, 40].

The population coverage of the vaccine candidate, derived from the integration of MHC-I and MHC-II binding epitopes, was notably high. COVID-19 disease has had a profound impact globally, particularly in the United States, Brazil, Europe, and India. The potential efficacy of the developed vaccine is underscored by its substantial predicted population coverage rates of 92.91%, 91.81%, 93.58%, and 89.55% for the United States, Brazil, Europe, and India, respectively. A comparative analysis with other vaccine candidates targeting similar populations, such as the mRNA-based vaccines, indicates that our approach could potentially offer broader coverage due to its inclusion of conserved epitopes across both SARS-CoV-2 and influenza [41]. Appropriate adjuvants and linkers were employed to facilitate the connection of the M2e, HA2, CTL, HTL, and BCR epitopes. Human β -defensin-2 (hBD-2) is recognized as a chemotactic agent for T-lymphocytes, monocytes, macrophages, and dendritic cells [42]. Furthermore, it plays a pivotal regulatory role in innate antiviral immunity and enhances the induction of antigen-specific immunity [43]. Consequently, hBD-2 was selected as an adjuvant at the N-terminal of our vaccine. The incorporation of adjuvants serves to prevent vaccine degradation, enhance immunogenicity, and regulate vaccine delivery [44]. Simultaneously, various linkers were integrated into the vaccine architecture to facilitate the connection of epitopes. In addition to their primary function of linking epitopes, linkers provide supplementary benefits, including the enhancement of biological activity, improvement of stability, and attainment of optimal conformations [45].

The vaccine construct was validated as non-allergenic and demonstrated favorable antigenic properties. Additionally, it was determined to be stable and soluble after expression in a bacterial system. The observed solubility of the vaccine can be attributed to the effective interaction between the exposed residues and their solvent-accessible regions. Conformational analysis revealed that 80% of the residues were exposed. Notably, the three-dimensional conformation of the vaccine displayed a well-structured design, characterized by appropriate Ramachandran values and Z-scores. Furthermore, conformational B-cell epitopes of the vaccine were identified. These epitopes consist of non-contiguous amino acid

sequences that collectively form an antigenic structure capable of interacting with B-cell receptors. Approximately 50% of the residues in the designed vaccine were found to be associated with conformational B-cell epitopes, indicating the potential for a robust antibody response post-vaccination. These findings are in line with similar studies that have shown the effectiveness of incorporating conformational B-cell epitopes to enhance vaccine immunogenicity [46]. Collectively, the diverse properties and analyses indicate that the constructed vaccine represents a promising candidate for combating COVID-19 and influenza infections.

The TLR-3, a member of the toll-like receptor family, is integral to pathogen recognition and the activation of innate immunity. TLR-3 is capable of recognizing components of coronaviruses, such as RNA and double-stranded RNA (dsRNA), thereby initiating an immune response aimed at eradicating the SARS-CoV-2 virus [47]. Additionally, TLR-3 function has been associated with influenza virus infections [48]. Molecular docking studies of the developed vaccine with the TLR-3 receptor demonstrated a significant propensity for interaction, indicating its potential efficacy in suppressing viral infection. Moreover, MD simulations demonstrated that the vaccine-TLR-3 complex maintained a compact and stable conformation throughout the simulation period. Further assessments indicated the thermal stability of the vaccine structure at low (4 °C), ambient (25 °C), and physiological (37.5 °C) temperatures, thereby facilitating its handling and storage. This stability at physiological temperature further substantiates the vaccine's robustness. Lastly, codon optimization was conducted to enhance expression efficiency and augment vaccine production within the *E. coli* expression system, with successful cloning serving as validation of this optimization.

Despite these promising findings, our study has certain limitations. First, the computational predictions, including antigenicity, allergenicity, and molecular docking analyses, rely on *in silico* tools, which, while highly informative, require experimental validation. Further *in vitro* and *in vivo* studies are necessary to confirm the immunogenicity and protective efficacy of the proposed vaccine. Second, while we employed multiple computational approaches to ensure vaccine stability and interaction with immune receptors, potential variations in real biological systems may impact the predicted outcomes. Finally, while the vaccine construct was optimized for expression in a bacterial system, alternative expression systems, such as yeast or mammalian cells, may need to be explored for enhanced production and efficacy [36, 49].

Conclusion

Vaccination plays a crucial role in the global control of COVID-19 and influenza infections, complementing pharmacological interventions and supportive care. In response to these challenges, a universal multi-epitope vaccine was developed using an immunoinformatics approach. This vaccine integrates CTL, BCR, HTL, M2e, and HA2 epitopes derived from the N protein of SARS-CoV-2 and the surface proteins of influenza viruses. Many of the selected epitopes have been validated for their immunogenicity through both in vivo and in vitro studies. The vaccine was found to be non-toxic, non-allergenic, highly soluble, and capable of achieving extensive population coverage. Additionally, it exhibited stability under cold, ambient, and physiological conditions. Importantly, the vaccine was shown to interact effectively with the TLR-3 immune receptor, and its expression was successfully confirmed in a bacterial host system. These findings underscore the vaccine's potential to elicit a robust immune response and provide broad protection against co-infections of COVID-19 and influenza globally.

Abbreviations

SARS-CoV-2	Severe acute respiratory syndrome Coronavirus 2
COVID-19	Coronavirus disease 2019
WHO	World Health Organization
ORFs	Open reading frames
sgRNAs	Subgenomic RNAs
MHC	Major histocompatibility complex
TLR-3	Toll-like receptor 3
MD	Molecular dynamics
M2e	Matrix-2 ectodomain
HA2	Hemagglutinin subunit 2
IgG	Immunoglobulin G
IEDB	Immune epitope database
CTL	Cytotoxic T lymphocyte
HTL	Helper T lymphocyte
BCR	B-cell receptor
VaxiJen	Vaccine antigenicity evaluation tool
TAP	Transporter associated with antigen processing
BepiPred	B-cell epitope prediction server
PDB	Protein data bank
PSIPRED	Protein secondary structure prediction
CAPRI	Critical assessment of predicted interactions
RMSD	Root mean square deviation
RMSF	Root mean square fluctuation
Rg	Radius of gyration
SASA	Solvent accessible surface area
H-bond	Hydrogen bond
PCA	Principal component analysis
DCCM	Dynamic cross-correlation matrix
FEL	Free energy landscape
NEBcutter	New England Biolabs cutter tool
pET-28a(+)	Expression plasmid with poly-histidine tag
6xHis-tag	Six histidine tag

Supplementary Information

The online version contains supplementary material available at <https://doi.org/10.1186/s12879-025-11066-3>.

Supplementary Material 1

Author contributions

S.M. and S.N.F. performed the laboratory experiments and collected the data. H.T. designed the study. S.M. and A.S. wrote the manuscript and performed the analysis. P.M. drew the graphs. All authors have confirmed and approved the study.

Funding

This research was financially supported by the Shahid Bahonar University Research Foundation in Kerman, Iran (Grant Number 9902097).

Data availability

The data that support the findings of this study are available from the corresponding authors as request.

Declarations

Ethics approval and consent to participate

Not applicable.

Consent for publication

Not applicable.

Competing interests

The authors declare no competing interests.

Author details

¹Department of Pathobiology, Faculty of Veterinary Medicine, Shahid Bahonar University of Kerman, Kerman, Iran

²Department of Clinical Science, Faculty of Veterinary Medicine, Shahid Bahonar University of Kerman, Kerman, Iran

³Faculty of Veterinary Sciences, Science and Research Branch, Islamic Azad University, Tehran, Iran

⁴Department of Animal Science, Faculty of Agriculture, University of Kurdistan, Sanandaj, Kurdistan, Iran

Received: 29 November 2024 / Accepted: 30 April 2025

Published online: 10 May 2025

References

- Harrington WN, Kackos CM, Webby RJ. The evolution and future of influenza pandemic preparedness. *Exp Mol Med*. 2021;53(5):737–49.
- Li P, Wang Y, Peppelenbosch MP, Ma Z, Pan Q. Systematically comparing COVID-19 with the 2009 influenza pandemic for hospitalized patients. *Int J Infect Dis*. 2021;102:375–80.
- Tufan A, Güler AA, Matucci-Cerinic M. COVID-19, immune system response, hyperinflammation and repurposing antirheumatic drugs. *Turk J Med Sci*. 2020;50(9):620–32.
- Girard MP, Tam JS, Assossou OM, Kiény MP. The 2009 A (H1N1) influenza virus pandemic: A review. *Vaccine*. 2010;28(31):4895–902.
- Saberi M, Tavakkoli H, Najmaddini A, Rezaei M. Serological prevalence of avian H9N2 influenza virus in dogs by hemagglutination inhibition assay in Kerman, southeast of Iran. In: *Veterinary Research Forum*. vol. 10; 2019: 249.
- Tavakkoli H, Asasi K, Mohammadi A. Effectiveness of two H9N2 low pathogenic avian influenza conventional inactivated oil emulsion vaccines on H9N2 viral replication and shedding in broiler chickens. *Iran J Veterinary Res*. 2011;12(3):214–21.
- Le TT, Andreadakis Z, Kumar A, Román RG, Tollefsen S, Saville M, et al. The COVID-19 vaccine development landscape. *Nat Rev Drug Discov*. 2020;19(5):305–6.
- Enayatkhani M, Hasaniazad M, Faezi S, Gouklani H, Davoodian P, Ahmadi N, et al. Reverse vaccinology approach to design a novel multi-epitope vaccine candidate against COVID-19: an in Silico study. *J Biomol Struct Dynamics*. 2021;39(8):2857–72.
- Golchin M, Moghadaszadeh M, Tavakkoli H, Ghanbarpour R, Dastmalchi S. Recombinant M2e-HA2 fusion protein induced immunity responses against intranasally administered H9N2 influenza virus. *Microb Pathog*. 2018;115:183–8.
- Singh A, Thakur M, Sharma LK, Chandra K. Designing a multi-epitope peptide based vaccine against SARS-CoV-2. *Sci Rep*. 2020;10(1):16219.

11. Cong Y, Ulasli M, Schepers H, Mauthe M, V'kovski P, Kriegenburg F, et al. Nucleocapsid protein recruitment to replication-transcription complexes plays a crucial role in coronavirus life cycle. *J Virol*. 2020;94(4):01925–19. <https://doi.org/10.1128/jvi.2020.01925>.
12. Leung DTM, Chi Hang TF, Chun Hung M, Sheung Chan PK, Cheung JLK, Niu H, et al. Antibody response of patients with severe acute respiratory syndrome (SARS) targets the viral nucleocapsid. *J Infect Dis*. 2004;190(2):379–86.
13. Dutta NK, Mazumdar K, Lee B-H, Baek M-W, Kim D-J, Na Y-R, et al. Search for potential target site of nucleocapsid gene for the design of an epitope-based SARS DNA vaccine. *Immunol Lett*. 2008;118(1):65–71.
14. Rani NA, Robin TB, Prome AA, Ahmed N, Moin AT, Patil RB, et al. Development of multi epitope subunit vaccines against emerging carp viruses cyprinid herpesvirus 1 and 3 using immunoinformatics approach. *Sci Rep*. 2024;14(1):11783.
15. Hebditch M, Carballo-Amador MA, Charonis S, Curtis R, Warwicker J. Protein-Sol: a web tool for predicting protein solubility from sequence. *Bioinformatics*. 2017;33(19):3098–100.
16. Yang J, Zhang Y. I-TASSER server: new development for protein structure and function predictions. *Nucleic Acids Res*. 2015;43(W1):W174–81.
17. Gopalakrishnan K, Sowmiya G, Sheik S, Sekar K. Ramachandran plot on the web (2.0). *Protein Pept Lett*. 2007;14(7):669–71.
18. Tavakkoli H, Imani M, Seyyed MR, Rezvani M. The effect of methenamine on vascular development: experimental investigation using in vivo and insilico methods. *Int J Reproductive Biomed*. 2020;18(8):579.
19. Santiago DN, Pevzner Y, Durand AA, Tran M, Scheerer RR, Daniel K, et al. Virtual target screening: validation using kinase inhibitors. *J Chem Inf Model*. 2012;52(8):2192–203.
20. Salari Z, Tavakkoli H, Khosravi A, Karamad E, Salarkia E, Ansari M, et al. Embryotoxicity of docosahexaenoic and eicosapentaenoic acids: in vivo and in Silico investigations using the chick embryo model. *Biomed Pharmacother*. 2021;136:111218.
21. Moin AT, Patil RB, Tabassum T, Araf Y, Ullah MA, Snigdha HJ, et al. Immunoinformatics approach to design novel subunit vaccine against the Epstein-Barr virus. *Microbiol Spectr*. 2022;10(5):e01151–22.
22. Moin AT, Rani NA, Patil RB, Robin TB, Ullah MA, Rahim Z, et al. In-silico formulation of a next-generation polyvalent vaccine against multiple strains of Monkeypox virus and other related poxviruses. *PLoS ONE*. 2024;19(5):e0300778.
23. Mustapha T, Zubair T, Patil RB, Bhongade BA, Sangshetti JN, Mali A, et al. In vitro and in Silico investigation of effects of antimicrobial peptides from Solanaceae plants against rice sheath blight pathogen rhizoctinia Solani. *PLoS ONE*. 2024;19(6):e0302440.
24. Petersen B, Lundegaard C, Petersen TN. NetTurnP—neural network prediction of beta-turns by use of evolutionary information and predicted protein sequence features. *PLoS ONE*. 2010;5(11):e15079.
25. Chauhan PK, Sowdhamini R. LIM domain-wide comprehensive virtual mutagenesis provides structural rationale for cardiomyopathy mutations in CSRP3. *Sci Rep*. 2022;12(1):3562.
26. Khan MT, Islam MJ, Parihar A, Islam R, Jerin TJ, Dhote R, et al. Immunoinformatics and molecular modeling approach to design universal multi-epitope vaccine for SARS-CoV-2. *Inf Med Unlocked*. 2021;24:100578.
27. Tavakkoli H, Khosravi A, Sharifi I, Salari Z, Salarkia E, Kheirandish R, et al. Partridge and embryonated Partridge egg as new preclinical models for candidiasis. *Sci Rep*. 2021;11(1):2072.
28. Kumari R, Kumar R, Consortium OSD, Lynn A. g_mmpbsa—A GRO-MACS tool for high-throughput MM-PBSA calculations. *J Chem Inf Model*. 2014;54(7):1951–62.
29. Musa MS, Islam MT, Billah W, Hossain MS, Rahat MSS, Bayil I, et al. Structure-based virtual screening of Trachyspermum ammi metabolites targeting acetylcholinesterase for Alzheimer's disease treatment. *PLoS ONE*. 2024;19(12):e0311401.
30. Kabsch W, Sander C. Dictionary of protein secondary structure: pattern recognition of hydrogen-bonded and geometrical features. *Biopolymers: Original Research on Biomolecules*. 1983;22(12):2577–637.
31. Lohia N, Baranwal M. An immunoinformatics approach in design of synthetic peptide vaccine against influenza virus. *Immunoinformatics*. 2020;229:43.
32. Song X, Li Y, Wu H, Qiu H-J, Sun Y. T-cell epitope-based vaccines: A promising strategy for prevention of infectious diseases. *Vaccines*. 2024;12(10):1181.
33. Pollard AJ, Bijker EM. A guide to vaccinology: from basic principles to new developments. *Nat Rev Immunol*. 2021;21(2):83–100.
34. Cuspoca AF, Diaz LL, Acosta AF, Peñaloza MK, Méndez YR, Clavijo DC, et al. An immunoinformatics approach for sars-cov-2 in Latam populations and multi-epitope vaccine candidate directed towards the world's population. *Vaccines*. 2021;9(6):581.
35. Sharma S, Kumari V, Kumbhar BV, Mukherjee A, Pandey R, Kondabagil K. Immunoinformatics approach for a novel multi-epitope subunit vaccine design against various subtypes of influenza A virus. *Immunobiology*. 2021;226(2):152053.
36. Arora S, Aryandra A. Epitope based vaccine designing—a mini review. *J Vaccines Immunol*. 2020;6:038–41.
37. Ezaj MMA, Junaid M, Akter Y, Nahrin A, Siddika A, Afrose SS, et al. Whole proteome screening and identification of potential epitopes of SARS-CoV-2 for vaccine design—an immunoinformatic, molecular Docking and molecular dynamics simulation accelerated robust strategy. *J Biomol Struct Dynamics*. 2022;40(14):6477–502.
38. Ghosh N, Sharma N, Saha I. Immunogenicity and antigenicity based T-cell and B-cell epitopes identification from conserved regions of 10664 SARS-CoV-2 genomes. *Infect Genet Evol*. 2021;92:104823.
39. Srivastava S, Verma S, Kamthania M, Kaur R, Badyal RK, Saxena AK et al. Structural basis to design multi-epitope vaccines against novel coronavirus 19 (COVID19) infection, the ongoing pandemic emergency: an in Silico approach. *BioRxiv*. 2020:2020.04. 01.019299.
40. Sadat SM, Aghadadeghi MR, Yousefi M, Khodaei A, Sadat Larjani M, Bahramali G. Bioinformatics analysis of SARS-CoV-2 to approach an effective vaccine candidate against COVID-19. *Mol Biotechnol*. 2021;63(5):389–409.
41. Khan K, Khan SA, Jalal K, Ul-Haq Z, Uddin R. Immunoinformatic approach for the construction of multi-epitopes vaccine against Omicron COVID-19 variant. *Virology*. 2022;572:28–43.
42. Duits LA, Ravensbergen B, Rademaker M, Hiemstra PS, Nibbering PH. Expression of β -defensin 1 and 2 mRNA by human monocytes, macrophages and dendritic cells. *Immunology*. 2002;106(4):517–25.
43. Kim J, Yang YL, Jang S-H, Jang Y-S. Human β -defensin 2 plays a regulatory role in innate antiviral immunity and is capable of potentiating the induction of antigen-specific immunity. *Viol J*. 2018;15:1–12.
44. Pulendran B, Arunachalam S, O'Hagan P. Emerging concepts in the science of vaccine adjuvants. *Nat Rev Drug Discovery*. 2021;20(6):454–75.
45. Chen X, Zaro JL, Shen W-C. Fusion protein linkers: property, design and functionality. *Adv Drug Deliv Rev*. 2013;65(10):1357–69.
46. Sun R, Qian MG, Zhang X. T and B cell epitope analysis for the immunogenicity evaluation and mitigation of antibody-based therapeutics. *MAbs*. Volume 16. Taylor & Francis; 2024. p. 2324836.
47. Astuti I. Severe acute respiratory syndrome coronavirus 2 (SARS-CoV-2): an overview of viral structure and host response. *Diabetes Metabolic Syndrome: Clin Res Reviews*. 2020;14(4):407–12.
48. Nakano T, Ohara Y, Fujita H, Ainai A, Yamamura E-T, Suzuki T, et al. Double-stranded structure of the polyinosinic-polycytidylic acid molecule to elicit TLR3 signaling and adjuvant activity in murine intranasal A (H1N1) pdm09 influenza vaccination. *DNA Cell Biol*. 2020;39(9):1730–40.
49. Deepthi V, Sasikumar A, Mohanakumar KP, Rajamma U. Computationally designed multi-epitope vaccine construct targeting the SARS-CoV-2 Spike protein elicits robust immune responses in Silico. *Sci Rep*. 2025;15(1):9562.

Publisher's note

Springer Nature remains neutral with regard to jurisdictional claims in published maps and institutional affiliations.